Kölliker–Fuse/parabrachial complex PACAP–glutamate pathway to the extended amygdala couples rapid autonomic and delayed endocrine responses to acute hypotension

Vito S. Hernández, Pedro D. Segura-Chama and Limei Zhang*

Dept. Physiology, School of Medicine, National Autonomous University of Mexico, Mexico City, Mexico
*Corresponding author: limei@unam.mx

Abstract

The calyx of Held is a giant axo-somatic synapse classically confined to the auditory brainstem. We recently identified morphologically similar calyx-like terminals in the extended amygdala (EA) that arise from the ventrolateral parabrachial complex and co-express PACAP, CGRP, VAChT, VGluT1, and VGluT2, targeting PKCδ+/GluD1+ EA neurons. Here we asked whether this parabrachial–EA pathway participates in compensation during acute hypotension. In rats given hydralazine (10 mg/kg, *i*.p.), we quantified Fos protein during an early phase (60 min) and a late phase (120 min). Early after hypotension, Fos surged in a discrete subpopulation of the parabrachial Kölliker–Fuse (KF) region and in the EA, whereas magnocellular neurons of the supraoptic and paraventricular nuclei (SON/PVN) remained largely silent. By 120 min, magnocellular SON/PVN neurons were robustly Fos-positive. Confocal immunohistochemistry showed that most Fos+ PKCδ/GluD1 EA neurons were encircled by PACAP+ perisomatic terminals (80.8%), of which the majority co-expressed VGluT1 (88.1%). RNAscope in situ hybridization further identified a selective KF population co-expressing Adcyap1 (PACAP) and Slc17a7 (VGluT1) that became Fos-positive during the early phase. Together these data indicate that a $KF^{PACAP/VGluT1}$ projection forms calyceal terminals around PKCδ/GluD1 EA neurons, providing a high-fidelity route for rapid autonomic rebound to falling blood pressure, while slower endocrine support is subsequently recruited via vasopressinergic magnocellular activation. This work links multimodal parabrachial output to temporally layered autonomic–neuroendocrine control.

Short abstract

Acute hypotension triggers rapid autonomic compensation followed by slower endocrine support. We identify a Kölliker–Fuse (KF) PACAP/VGluT1 pathway to the extended amygdala (EA) that initiates the fast limb. In hydralazine-treated rats, Fos rose at 60 min in KF and EA but not in magnocellular SON/PVN; by 120 min SON/PVN were strongly Fos-positive. Confocal microscopy showed that ~81% of Fos+ PKCδ/GluD1 EA neurons were surrounded by PACAP+ calyceal terminals, ~88% of which co-expressed VGluT1. RNAscope revealed a selective KF

Adcyap1/Slc17a7 population that became Fos-positive early. We conclude that KF PACAP/VGluT1 calyces onto PKCδ/GluD1 EA neurons provide a high-fidelity autonomic pathway that precedes vasopressin-mediated endocrine compensation.

Introduction

The extended amygdala (EA), comprising the capsular division of the central amygdala (CeC) and the oval nucleus of the bed nucleus of the stria terminalis (BSTov), is a hub for rapid viscerosensory integration and for coordinating autonomic, behavioral, and emotional responses to threats and homeostatic challenges (Goehler 2011, Crestani, Alves et al. 2013). These nuclei receive dense inputs from brainstem centers that relay visceral and nociceptive signals - most notably the parabrachial nucleus (PBN)—which alert the EA to internal bodily states and imminent threats (Takeuchi, Xie et al. 2004, Jaramillo, Brown et al. 2021). In turn, the CeC and BSTov project to hypothalamic and medullary effectors to orchestrate defensive and stress-related responses; for example, the central amygdala modulates freezing, startle, and autonomic adjustments, including heart-rate and blood-pressure changes, via projections to the rostral ventrolateral medulla (RVLM) and hypothalamus (Radke 2009). Rapid excitation of CeC neurons, which disinhibit downstream sympatho-excitatory pathways, is therefore well positioned to influence blood-pressure (BP) control.

We recently identified a multimodal calyceal synapse in the EA (Zhang, Hernández et al. 2025) formed by PACAP-expressing neurons of the Kölliker–Fuse (KF) nucleus, a ventrolateral subdivision of the parabrachial complex (Zhang, Hernandez et al. 2021, Zhang, Hernández et al. 2025). These giant axo-somatic terminals co-package glutamate, acetylcholine, and multiple neuropeptides, enveloping PKCδ^{+}/GluD1^{+} neurons in the CeC and BSTov. Confocal microscopy, focused-ion-beam scanning electron microscopy (FIB-SEM), and 3-D reconstructions confirmed multiple synaptic specializations onto this PKCδ^{+} subpopulation. The terminals co-express VGluT1, VGluT2, VAChT, PACAP, CGRP, neurotensin, and calretinin, whereas the postsynaptic targets express GluD1, a synaptic adhesion molecule implicated in stabilizing large glutamatergic contacts (Dai, Patzke et al. 2021, Liakath-Ali, Polepalli et al. 2022), suggesting convergence of excitatory, cholinergic, and peptidergic signaling at a single high-fidelity axo-somatic interface.

Located near the pontine–mesencephalic junction, the KF has long been recognized as part of the pontine respiratory ("pneumotaxic") network that shapes respiratory rhythm and phase transitions and contributes to upper-airway and autonomic control (Varga et al., 2021; Toor et al., 2024; Geerling et al., 2017). Its PACAP- and glutamate-expressing neurons position the KF to integrate sensory signals with autonomic output (Eiden 2021, Zhang, Hernandez et al. 2021).

Here, using a hydralazine-induced acute hypotension model in rats, we show that the KF to CeC/BSTov calyceal pathway is rapidly recruited during the early phase of BP recovery, independently of hypothalamic magnocellular activation. We propose a two-tiered compensation: a fast, high-fidelity K to EA drive that reinstates sympathetic tone, followed by slower hypothalamo–neurohypophysial support that sustains BP stabilization.

Results and discussion

Pioneering work had hinted that parabrachial complex to CeC pathway is recruited during acute hypotension (Takeuchi, Xie et al. 2004). To assess the physiological implications of the functional recruitment of KF to EA pathway, we used the hydralazine (HDZ)-induced acute hypotension (Graham, Hoffman et al. 1995) for probing this pathway's involvement in BP restoration.

The systemic administration of hydralazine (HDZ; 10 mg/kg, i.p. single injection) produced a robust fall in arterial blood pressure (ABP) during the first 60 mins. Averaged mean arterial pressure (MAP) recordings obtained using the CODA HT noninvasive BP system (saline vs HDZ) are shown in the figure 1. The mean ABP fell from 110.8 ± 2.5 mmHg to 82.8 ± 3.9 mmHg within the first 5 mins and continued to 68.9 ± 6.4mmHg at the 10 min time point. The mean ABP restored gradually (the significant difference disappeared at 90 min time-point after HDZ injection, 98.2 ± 6.9 mmHg).

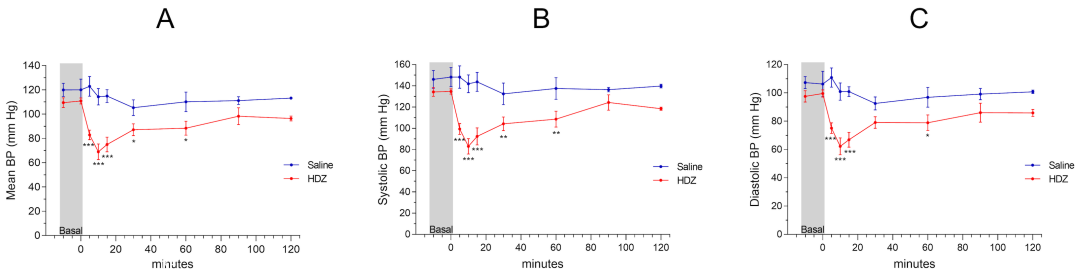

Figure 1 Blood pressure dynamic change as a function of one systemic (intraperitoneal i.p.) hydralazine administration. A. Time course of mean blood pressure (BP) changes measured between 10 min before the i.p. injection (t = 0) to 120 min after the injection. B and C, time courses of systolic and diastolic blood pressure (BP) changes respectively (N = 6, n=3). * P < 0.05; ** P < 0.01; ***P < 0.001. Two-way ANOVA followed by Fisher's LSD multiple comparisons test.

With the acute HDZ hypotensive effect validated, we sought to identify the brain regions engaged during the compensatory response to hypotension, we mapped Fos immunoreactivity at 60 min ("early-Fos") and 120 min ("late-Fos") after HDZ injection (Fig. 2A). At 60 min, a distinct

subpopulation within the ventrolateral parabrachial complex—the Kölliker–Fuse nucleus (KF)—showed robust Fos induction, together with strong labeling in the capsular central amygdala (CeC) and oval BNST (BSTov) (Fig. 2B3–D3). In contrast, magnocellular neurons of the supraoptic (SON) and paraventricular (PVN) nuclei remained largely quiescent at this time point (Fig. 2E2). By 120 min, however, the SON and PVN exhibited dense nuclear Fos expression (Fig. 2E4), marking a late phase of activation. Quantitative analyses confirmed a significant increase in Fos-positive cell density in KF, CeC, and BSTov at 60 min, followed by pronounced labeling in PVN/SON at 120 min (Fig. 2F; one-way ANOVA, different letters = $p < 0.05$). These results delineate a two-stage temporal pattern: an early activation of the KF → EA network that precedes a later recruitment of hypothalamo-neurohypophysial neurons responsible for vasopressin release.

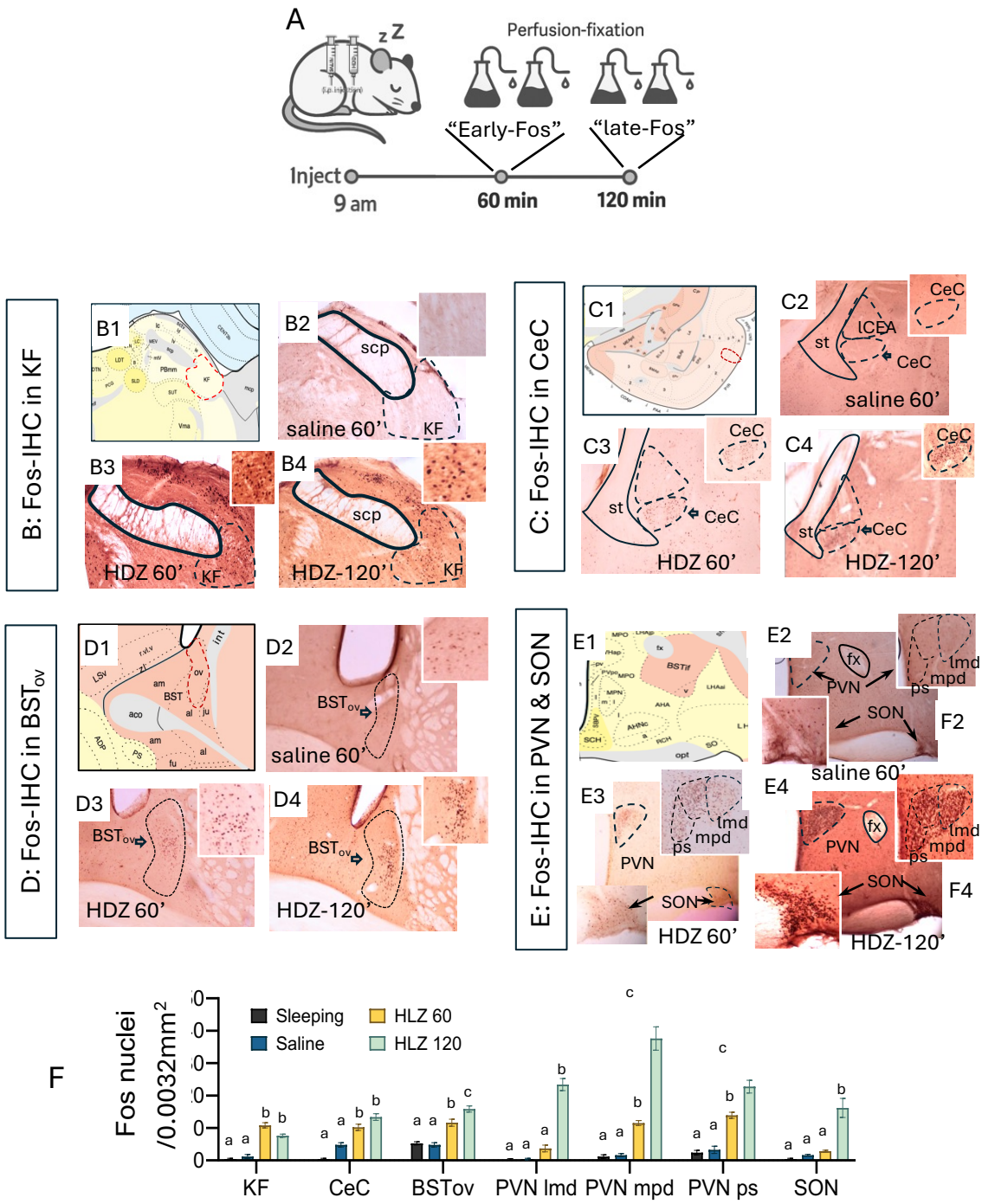

Figure 2. Sequential Fos activation of brainstem KF, extended amygdala and hypothalamic PVN/SNO parvo and magnocellular neuronal populations. A) Cartoon represent the experimental design where 4 experimental groups of rats participated. At 9am while most of rats were sleeping in their cages, were awakened by injecting: a) "sleeping" group: pentobarbital for subsequent perfusion/fixation, b) "saline" group: saline (0.9% NaCl, 1ml/kg), c) "early-" and d) "late-" phase of Fos groups: HDZ (10mg/kg, in saline 1ml/kg). Groups b and c were anesthetized and perfused/fixed at 60 min time point while the group d) was processed at 120 min. B-E: Panels "1": Swanson's rat brain map levels corresponding C1, Kölliker-Fuse nucleus (KF, ventral subdivision of the parabrachial complex), D1, central amygdala, capsular subdivision CeC, E1, bed nucleus of stria terminalis, oval subdivision (BSTov) and E1, supraoptic hypothalamus. Panels "2", Fos expression patterns of the 4 regions from the saline group; panels "3": Fos expression patterns of the 4 regions from the HDZ 60 group; panels "4": Fos expression patterns of the 4 regions from the HDZ 120 group. G) Quantification of Fos+ cell densities of 4 experimental groups: a): "sleeping" and "saline" groups, n=3, c, n=5, and d, n=6. Different lettering indicate significant statistical differences.

To determine the cellular targets activated during the early phase, we combined Fos immunofluorescence with markers of the calyceal input previously described in the extended amygdala. At 60 min post-HDZ, numerous Fos-positive nuclei were observed within the CeC, surrounded by ring-like PACAP-immunoreactive terminals (Fig. 3A). High-resolution confocal imaging revealed that these perisomatic rings correspond to VGluT1^{+}/PACAP^{+} axo-somatic structures apposed to PKCδ^{+} neurons (Fig. 3B). Many of these terminals also contained CGRP and formed contacts adjacent to GluD1-positive postsynaptic domains (Fig. 3C,D). Quantitative analysis showed that 80.8 % of Fos-positive neurons were surrounded by PACAP^{+} calyceal terminals and 88.1 % of these perisomatic rings co-expressed VGluT1 (Fig. 3E,F). These data demonstrate that the PACAP/VGluT1 calyceal input to PKCδ/GluD1 CeC neurons is selectively engaged during the early compensatory phase of acute hypotension.

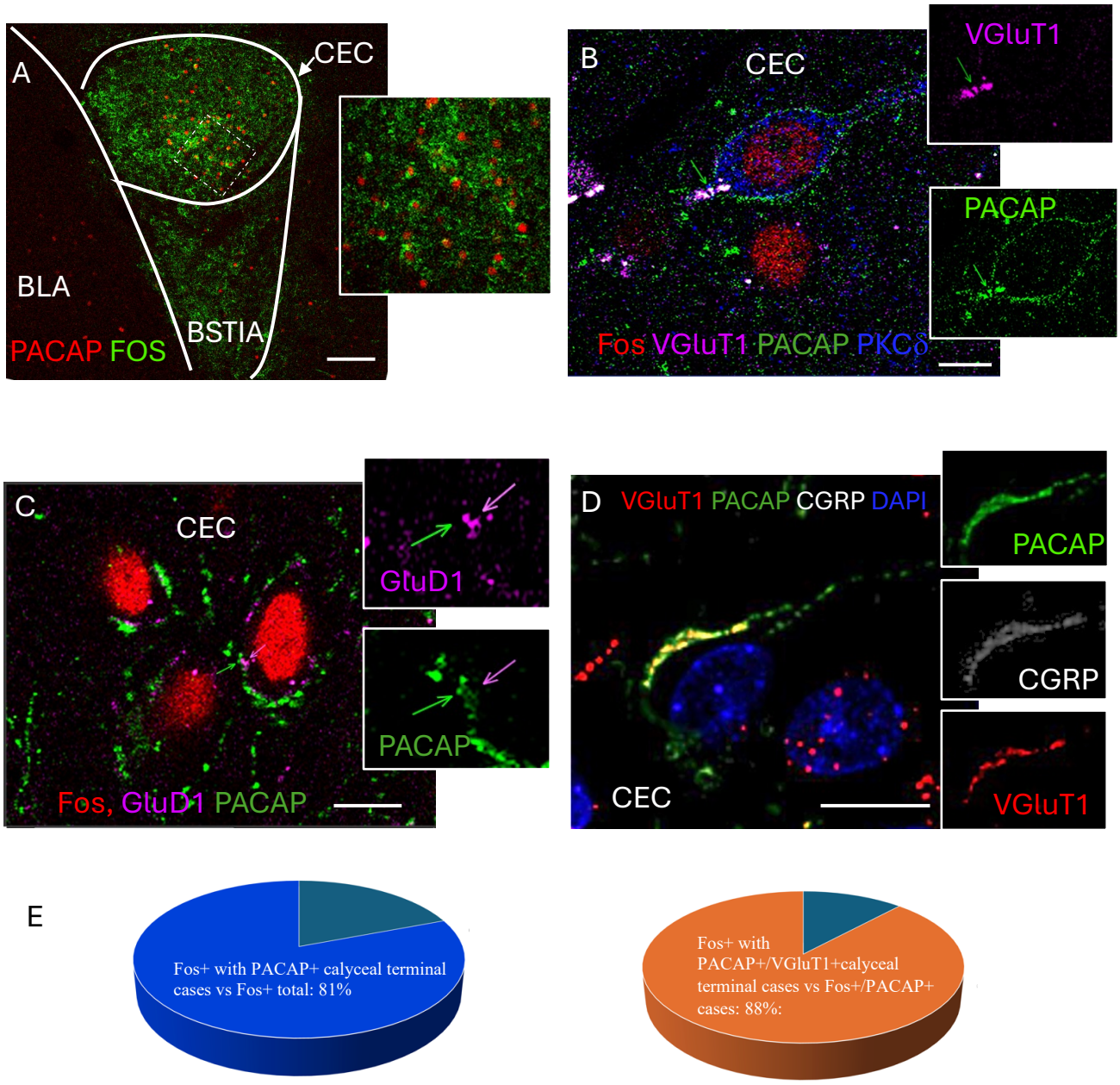

Figure 3. Fos assessed at the early phase demonstrating the selective activation of the calyceal synapse targeting neurons. A. low magnification micrograph showing the Fos expressing neurons in the CEC (inset showing the Fos expressing nuclei surrounded by PACAP-ir ringlike structure. B-D: thin-confocal micrographs (1 Airy: 1mm) showing B, a PKCd-ir (blue) cell, which expressed Fos at the early phase, targeted by PACAP/VGluT1 co-expressing calyceal structure, C. the PACAP axon was apposed by GluD1-ir puncta in the cytoplasm side, D. the PACAP-ir calyceal axon terminal co-expressed CGRP and VGluT1. Scale bars: A: 100µm, B-D: 10µm. E and F, pie charts represent the percentage of Fos+ neurons with PACAP+ calyceal axon terminal surrounding vs in total Fos expressing cells (E: 42 in 52 cases, 80.796%) and of Fos+ neurons with PACAP+/VGluT1+ calyceal axon terminal surrounding vs in total Fos/PACAP cases (F: 37 in 42 cases, 88.095%).

To identify the upstream neurons giving rise to the PACAP/VGluT1 calyceal terminals, we examined gene expression in the KF using single- and duplex-RNAscope in situ hybridization. Adcyap1 (PACAP mRNA)-positive neurons formed a dense cluster within the ventrolateral parabrachial complex (Fig. 4A), and many also expressed Slc17a7 (VGluT1 mRNA; Fig. 4B,E). Duplex assays combining Fos with Adcyap1 or Slc17a7 revealed that a subpopulation of PACAP^{+}/VGluT1^{+} KF neurons became Fos-positive at 60 min following HDZ (Fig. 4C,D). Additional duplex reactions confirmed partial co-expression of Adcyap1 and Calca (CGRP) (Fig. 4F), consistent with the mixed neurochemical profile of the calyceal terminals in the CeC. Together, these data identify a discrete PACAP/VGluT1-expressing KF subpopulation that is activated during the early phase of hypotensive challenge and likely constitutes the source of the PACAPergic calyceal projection to the extended amygdala.

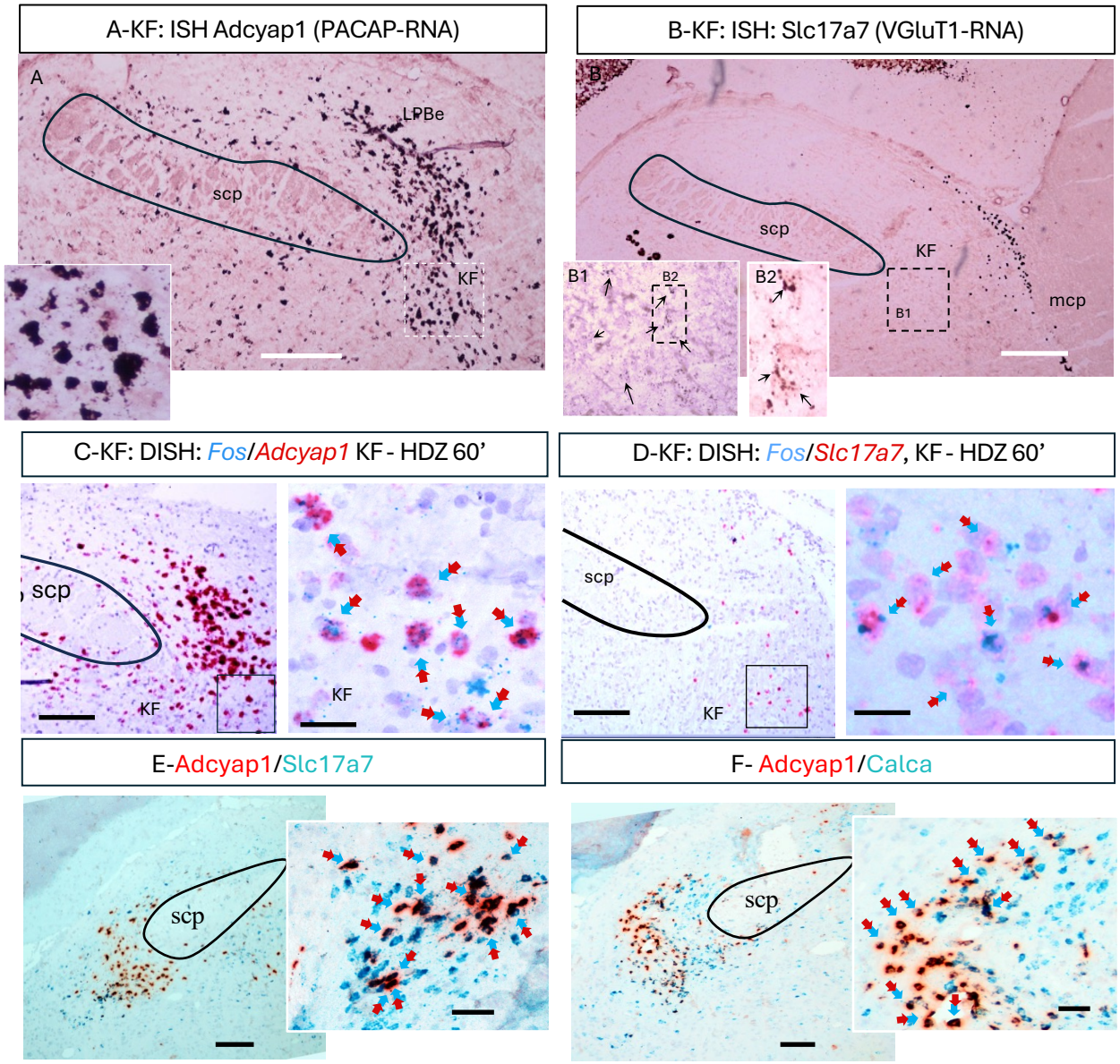

Figure 4 A subpopulation in the pontine Kölliker-Fuse nuclei (KF) which expressed mRNA of PACAP/VGluT1 engaged in the early phase of the acute hypotension event. A and B: ISH using high sensitivity/low background single cell labeling with RNAscope brown-kit method revealed a peculiar cell population of rat brain located in the ventral subdivision of the pontine parabrachial complex, at bregma -9.12mm to - 9.24mm, medio-lateral 2.90mm - 3.00mm and dorso-ventral 7.40mm to 7.60mm, between the superior and medial cerebellar peduncles (scp and mcp, respectively), with large cell bodies, expressing Adcyap1 (mRNA for PACAP, panel A and inset) and Slc17a7 (mRNAs for VGluT1, panel B and inset, where the Slc17a7 positive grains can be clearly seen on and surround the Nissl stained nuclei, white arrows). C and D: with RNAscope duplex method (DISH) it is evident that this $KF^{PACAP/VGluT1}$ population is fos positive at the early raising phase. E and F, DISH reactions show the co-expression of Adcyap1 (PACAP) co-expressing Slc17a7 (VGluT1) and Calca (CGRP). Scale bars: A and B, 200µm, C-F: left panels, 50µm, right panels: 25µm.

Discussion

Our findings reveal a previously unrecognized synaptic mechanism that couples a rapid autonomic response with a delayed neuroendocrine compensation after acute hypotension. The identification of a PACAP/VGluT1/CGRP calyceal projection from the Kölliker–Fuse (KF) nucleus to $PKC\delta^+$/$GluD1^+$ neurons of the extended amygdala (EA) introduce a new element into the organization of central networks that control blood pressure. This discovery expands the classical model of cardiovascular homeostasis beyond medullary baroreflex circuits, incorporating a high-fidelity pontine–amygdaloid route capable of influencing sympathetic outflow with exceptional temporal precision.

The biphasic Fos pattern observed i.e. early activation in the KF and EA followed by delayed recruitment of vasopressinergic magnocellular neurons, suggests a two-stages temporal hierarchy in the brain's response to falling blood pressure. In the first stage, PACAP/VGluT1/CGRP calyceal input rapidly excites $PKC\delta^+$ neurons in CeC and BSTov, which are strategically positioned to modulate sympathoexcitatory outputs through disinhibition of hypothalamic and medullary targets (Crestani, Alves et al. 2013, Son, Filosa et al. 2013). This fast relay may provide the neural substrate for the "autonomic rescue" phase, restoring arterial pressure before endocrine mechanisms become engaged. The second delayed stage, engages magnocellular SON/PVN neurons to ensure sustained vasopressin-mediated volume recovery and allostatic stabilization (Leng and Russell 2019).

The calyx-like terminals described here resemble those of the auditory brainstem in scale and transmitter complexity, but they occur in a forebrain circuit governing visceral / autonomic state rather than sound localization. Their morphology and multi-transmitter composition imply exceptionally reliable transmission with the potential for graded modulation by neuropeptides. PACAP, co-released with glutamate, likely enhances presynaptic Ca^{2+} influx and postsynaptic

excitability, thus amplifying the gain of the autonomic response (Zhang, Hernandez et al. 2021). The co-presence of VAChT in these PACAP/CGRP terminals, suggests synergistic recruitment of peptidergic and cholinergic modulation, conferring both precision and persistence. Functionally, this arrangement may enable the EA to detect visceral perturbations not merely as sensory inputs but as urgent salience signals requiring rapid autonomic adjustment.

By positioning the EA as a recipient of KF autonomic drive, our results bridge two traditionally distinct domains viscerosensory control and emotional processing. The same PKCδ^{+} EA neurons involved in hypotensive compensation also regulate fear and anxiety states (Duvarci, Bauer et al. 2009, Duvarci and Pare 2014, Hevesi, Zelena et al. 2021) Thus, the calyceal pathway could represent an anatomical substrate through which internal bodily challenges engage affective circuits, giving rise to the subjective awareness of "bodily threat" (Critchley, Mathias et al. 2002). The dual role of PACAP in both stress (Stroth, Holighaus et al. 2011, Zhang and Eiden 2019) and cardiovascular regulation (Dalsgaard, Hannibal et al. 2003) supports this idea: PACAP signaling in the amygdala and BNST has been implicated in anxiety and panic disorders (Missig, Mei et al. 2017, Li, Andero et al. 2023). Our data therefore offer a mechanistic framework for understanding how visceral disturbances can trigger emotional arousal, unifying autonomic and affective physiology.

This study introduces the first direct evidence of a multimodal calyceal synapse operating within a limbic–autonomic network. Beyond hypotension, such architecture may contribute to cardiorespiratory coupling during hypoxia (Toor, Burke et al. 2024) or to stress-induced sympathetic activation (Damasceno, Takakura et al. 2015). Future electrophysiological work would be key to determine whether PACAP-dependent facilitation at these terminals shows activity-dependent plasticity, potentially explaining persistent sympathetic bias in chronic stress or hypertension. Likewise, identifying homologous KF to EA pathways in humans (Lavezzi, Ottaviani et al. 2004)may clarify the neural basis of dysautonomic states and anxiety-related cardiovascular symptoms.

Limitations and future directions

Our study is correlative with respect to causality: we infer the pathway's contribution from Fos mapping and anatomical convergence. Direct tests will require temporally precise inhibition or activation of KF PACAP/VGluT1 neurons and selective disruption of EA calyces (e.g., synaptotagmin manipulation, targeted peptide receptor blockade). Continuous telemetry would complement tail-cuff measures to capture second-to-second dynamics. Finally, identifying the downstream EA efferents that mediate sympathetic rebound (e.g., projections to RVLM or hypothalamic premotor areas) will clarify the effector arm.

Conclusion

We define a KF PACAP/VGluT1 projection that forms calyceal terminals onto PKCδ/GluD1 neurons in the extended amygdala and is selectively engaged during the early phase of recovery from acute hypotension. This pathway provides a mechanistic substrate for rapid autonomic compensation that precedes and complements slower vasopressin-dependent endocrine support, revealing a temporally stratified architecture for cardiovascular homeostasis.

Materials and methods

Adult (>60 days) male Wistar rats were obtained from the vivarium of the School of Medicine, National Autonomous University of Mexico. Rats were housed under controlled temperature and humidity on a 12-h light cycle (lights on at 07:00, off at 19:00) with ad libitum access to standard chow and water. All procedures were approved by the School of Medicine's Ethics Committee (License: CIEFM-079-2020).

Blood Pressure Measurements.

The blood pressure (BP) measurements in conscious rats were done between 10:00 a.m. and 03:00 p.m. via a non-invasive tail-cuff CODA system (Kent Scientific Corp., USA). Animals were acclimated to restraining device and the sensing tail-cuff during 30 min to avoid unnecessary stress in the course of measurements. During recording, the occlusion cuff and the volume pressure recording (VPR) sensor was positioned on the tail base while the rats were maintained in a heater platform set to 30 °C to induce vasodilation, which enhances the blood flow to the tail. Data of BP (the average of 3 times) were evaluated two times at basal level and 5, 10, 15, 30 and 60, 90 and 120 minutes after hydralazine (10 mg/Kg-1) or saline (0.9 % NaCl, 1 mL/Kg-1) intraperitoneal administration. CODA software displays the systolic, diastolic and mean blood pressure data in mmHg units. Data are expressed as mean ± SEM of BP measurements in mmHg of at least 3 rats per condition and indicated time. Statistical analysis was performed using two-way ANOVA followed by Fisher's LSD multiple comparisons post hoc test, a statistically significant difference was set with a P value < 0.05.

Immunohistochemistry for light microscopy. Rodents were perfused via the ascending aorta with 0.9% NaCl followed by 4% paraformaldehyde. Brains were sectioned at 70 µm using a Leica VT1200 vibratome. Sections were washed in phosphate buffer (PB), blocked for 2 hours in TBST (0.05 M Tris, 0.9% NaCl, 0.3% Triton-X) plus 10% normal donkey serum, and incubated overnight at 4°C with primary antibodies (see SI table 1 diluted in TBST with 1% serum. After washing, sections were incubated for 2 hours at room temperature with appropriate biotinylated or

fluorescent secondary antibodies (1:500; Vector Laboratories). Brightfield images were acquired using a Nikon Eclipse E600, and confocal images were acquired with a Leica Stellaris microscope.

Primary antibodies

Target	Host Species	Dilution	Source	Catalog Number
PACAP	Rabbit	1:2000	BMA	T-4473
VGluT1	Guinea pig	1:5000	Chemicon	AB-5905
CGRP	Rabbit	1:1000	Phoenix Pharmaceuticals	H-015-09
Fos	Rabbit	1:2000	EnCor	Cat# RPCA-c-FOS
GluD1	Guinea Pig	1:1000	Frontier Institute	GluD1C-GP-Af860
PKC∂	Mouse	1:1000	BD-Transduction Labs	610397

RNAscope In Situ Hybridization. rat brains were rapidly dissected, flash-frozen, and stored at −80 °C. Coronal sections (12 µm) were cut at −20 °C and mounted onto slides. RNAscope was performed using manufacturer instructions (Advanced Cell Diagnostics). Sections were fixed, dehydrated, and treated with Protease IV before hybridization with target probes at 40 °C for 2 h. The following probes were used: Adcyap1, Slc17a7, Slc17a6, and Calca. After hybridization, slides were washed, amplified, counterstained with DAPI, and coverslipped. Imaging was performed using a Leica Stellaris confocal microscope with a 20× objective.

Author Contributions: LZ, VSH conceived and designed the study. LZ, VSH, PDSC performed experiments and collected data. LZ secured funding and wrote the original draft. All authors have read and approved the final version of the manuscript.

Acknowledgements

This research was supported by funding from the following sources: the National Autonomous University of Mexico (UNAM-PAPIIT-IG200121); the Mexican Secretaría de Ciencias, Humanidades, Tecnología e Innovación (Secihti, CF-2023-G-243). We thank Lee Eiden for reagents support and Edgar Jiménez Díaz for technical support.

References

Crestani, C. C., F. H. Alves, F. V. Gomes, L. B. Resstel, F. M. Correa and J. P. Herman (2013). "Mechanisms in the bed nucleus of the stria terminalis involved in control of autonomic and neuroendocrine functions: a review." Curr Neuropharmacol **11**(2): 141–159.

Critchley, H. D., C. J. Mathias and R. J. Dolan (2002). "Fear conditioning in humans: the influence of awareness and autonomic arousal on functional neuroanatomy." Neuron **33**(4): 653–663.
Dai, J., C. Patzke, K. Liakath-Ali, E. Seigneur and T. C. Sudhof (2021). "GluD1 is a signal transduction device disguised as an ionotropic receptor." Nature **595**(7866): 261–265.
Dalsgaard, T., J. Hannibal, J. Fahrenkrug, C. R. Larsen and B. Ottesen (2003). "VIP and PACAP display different vasodilatory effects in rabbit coronary and cerebral arteries." Regul Pept **110**(3): 179–188.
Damasceno, R. S., A. C. Takakura and T. S. Moreira (2015). "Respiratory and sympathetic chemoreflex regulation by Kolliker-Fuse neurons in rats." Pflugers Arch **467**(2): 231–239.
Duvarci, S., E. P. Bauer and D. Pare (2009). "The bed nucleus of the stria terminalis mediates inter-individual variations in anxiety and fear." J Neurosci **29**(33): 10357–10361.
Duvarci, S. and D. Pare (2014). "Amygdala microcircuits controlling learned fear." Neuron **82**(5): 966–980.
Eiden, L. E., Hernandez, V.H., Jiang, S.Z., Zhang, L. (2021). Functional Chemoanatomy of PACAP in Neuroendocrine and NeuronalCircuits. Neuroanatomy of Neuroendocrine Systems. Á. D. Valery Grinevich. Switzerland, Springer**:** 429 – 487.
Goehler, L. (2011). Vicerosensory pathway in the brain. The science and clinical application of manual therapy. H. King, J. W and M. Patterson. Edinburgh, Churchill Livingston Elsevier**:** 163–179.
Graham, J. C., G. E. Hoffman and A. F. Sved (1995). "c-Fos expression in brain in response to hypotension and hypertension in conscious rats." J Auton Nerv Syst **55**(1-2): 92–104.
Hevesi, Z., D. Zelena, R. A. Romanov, J. Hanics, A. Ignacz, A. Zambon, D. D. Pollak, D. Lendvai, K. Schlett, M. Palkovits, T. Harkany, T. G. M. Hokfelt and A. Alpar (2021). "Secretagogin marks amygdaloid PKCdelta interneurons and modulates NMDA receptor availability." Proc Natl Acad Sci U S A **118**(7).
Jaramillo, A. A., J. A. Brown and D. G. Winder (2021). "Danger and distress: Parabrachial-extended amygdala circuits." Neuropharmacology **198**: 108757.
Lavezzi, A. M., G. Ottaviani, L. Rossi and L. Matturri (2004). "Cytoarchitectural organization of the parabrachial/Kolliker-Fuse complex in man." Brain Dev **26**(5): 316–320.
Leng, G. and J. A. Russell (2019). "The osmoresponsiveness of oxytocin and vasopressin neurones: Mechanisms, allostasis and evolution." J Neuroendocrinol **31**(3): e12662.
Li, Y., R. Andero, N. V. Luchkina, J. Suh, R. A. Ross, B. B. Lowell, W. A. Carlezon, K. J. Ressler and V. Y. Bolshakov (2023). "PACAP-mediated gating of anxiety-controlling circuits." bioRxiv.
Liakath-Ali, K., J. S. Polepalli, S. J. Lee, J. F. Cloutier and T. C. Sudhof (2022). "Transsynaptic cerebellin 4-neogenin 1 signaling mediates LTP in the mouse dentate gyrus." Proc Natl Acad Sci U S A **119**(20): e2123421119.
Missig, G., L. Mei, M. A. Vizzard, K. M. Braas, J. A. Waschek, K. J. Ressler, S. E. Hammack and V. May (2017). "Parabrachial Pituitary Adenylate Cyclase-Activating Polypeptide Activation of Amygdala Endosomal Extracellular Signal-Regulated Kinase Signaling Regulates the Emotional Component of Pain." Biol Psychiatry **81**(8): 671–682.
Radke, A. K. (2009). "The role of the bed nucleus of the stria terminalis in learning to fear." J Neurosci **29**(49): 15351–15352.
Son, S., J. Filosa, E. Potapenko, V. Biancardi, H. Zheng, K. Patel, V. Tobin, M. Ludwig and J. Stern (2013). "Dendritic Peptide Release Mediates Interpopulation Crosstalk between Neurosecretory and Preautonomic Networks." Neuron **78**: 1036–1049.
Stroth, N., Y. Holighaus, D. Ait-Ali and L. E. Eiden (2011). "PACAP: a master regulator of neuroendocrine stress circuits and the cellular stress response." Ann N Y Acad Sci **1220**(1): 49–59.

Takeuchi, Y., Q. Xie, T. Miki, Y. Matsumoto, I. Satriotomo, H. P. Li and H. Gu (2004). "Parabrachial inputs to Fos-immunoreactive neurons in the lateral central nucleus of amygdala activated by hypotension: a light and electron microscopic study in the rat." Brain Res Bull **64**(2): 171–180.
Toor, R., P. G. R. Burke, B. Dempsey, Q. J. Sun, C. M. Hildreth, J. K. Phillips and S. McMullan (2024). "Role of the Kolliker-Fuse/parabrachial complex in the generation of postinspiratory vagal and sympathetic nerve activities and their recruitment by hypoxemic stimuli in the rat." J Neurophysiol **132**(5): 1496–1506.
Zhang, L., V. S. Hernandez, C. R. Gerfen, S. Z. Jiang, L. Zavala, R. A. Barrio and L. E. Eiden (2021). "Behavioral role of PACAP signaling reflects its selective distribution in glutamatergic and GABAergic neuronal subpopulations." Elife **10**.
Zhang, L., V. S. Hernández, D. M. Giraldo, J. C. León-Contreras, R. Ye, S. Zhang, M. K.-H. Schäfer, R. A. Barrio, R. Hernández-Pando, F. Ferraguti and L. E. Eiden (2025). "Novel multi-transmitter calyx-like giant synapse revealed in the extended amygdala." bioRxiv: 2025.2004.2003.647119.
Zhang, L. M. and L. E. Eiden (2019). "Two ancient neuropeptides, PACAP and AVP, modulate motivated behavior at synapses in the extrahypothalamic brain: a study in contrast." Cell and Tissue Research **375**(1): 103–122.